

# Statistics of contribution of energetic electron precipitations: ELFIN and DMSP observations

Zijin Zhang, Anton V. Artemyev, Vassilis Angelopoulos  
University of California, Los Angeles

## Introduction - Energetic Electron Precipitation

Energetic electron precipitation couples magnetosphere and ionosphere  
DMSP provides low-energy measurements (30 keV) ELFIN extends to higher energies (50 keV to 6 MeV)

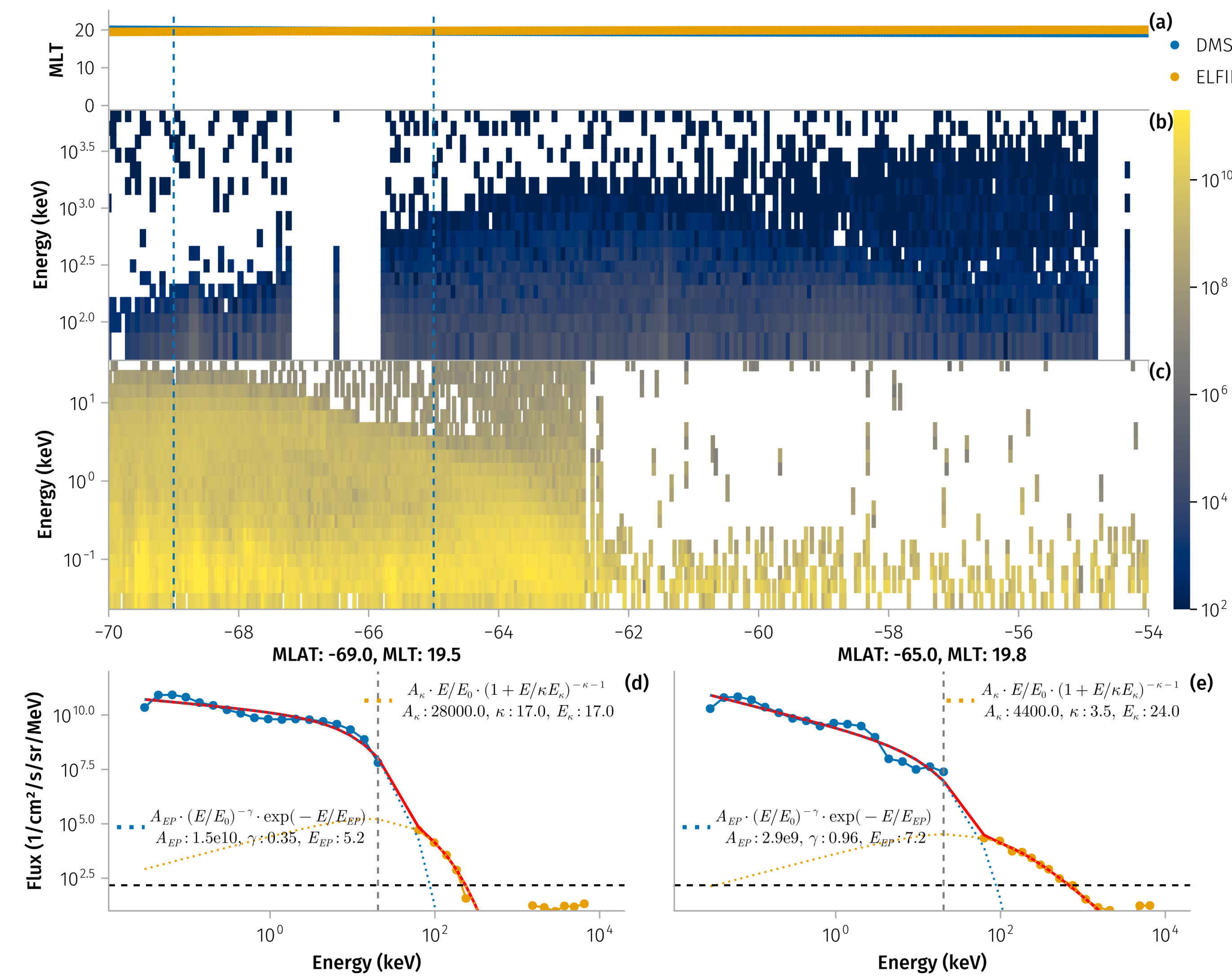


Figure 1: Example of a satellite conjunction event observed between 2021-12-01T22:19 and 2021-12-01T22:28. Panels (a-c) are plotted against magnetic latitude (MLAT): (a) the magnetic local time (MLT); (b) the precipitating electron flux measured by ELFIN; and (c) the electron flux measured by DMSP. Panels (d-e) display the precipitating flux spectra from both satellites, averaged over  $0.5^\circ$  MLAT bins.

## Model - Predict Precipitating Electron Flux

Final products: 1. Event catalog and 2. empirical, data-driven model.

```
using DEEEP # DmspElfinEnergeticElectronPrecipitation
```

```
model = load_flux_model()
```

```
# Evaluate flux at specific geophysical conditions: Location: 65° MLAT,  
6 MLT (dawn sector), Activity: Moderate (AE = 150 nT)
```

```
j_Efunc = model(; mlat=65.0, mlt=6.0, ae=150.0)
```

```
E = 10.0 # [keV]
```

```
flux_10keV = j_Efunc(E) # Calculate flux at a specific energy
```

```
energies = 10.^ range(log10(0.03), log10(1000), length=100) # 0.03 -  
1000 keV
```

```
spectrum = j_Efunc.(energies) # Generate the full energy spectrum
```

## Results - MLAT-MLT-AE Dependence

Our analysis reveals that energetic flux, number flux, average energy and kappa parameter exhibit a strong dependence on MLAT, MLT, and geomagnetic activity.

- The strongest energy and number fluxes occur in the **dawn** sector at high magnetic latitudes ( $65^\circ$ – $75^\circ$ ), the relative contribution of energetic particles exhibits an **anti-correlated** behavior.
- The energetic ( $> 30$  keV) component makes a substantial contribution to the total energy flux in the **dusk** sector, emphasizing the importance of accounting for this population to accurately characterize magnetosphere-ionosphere coupling.

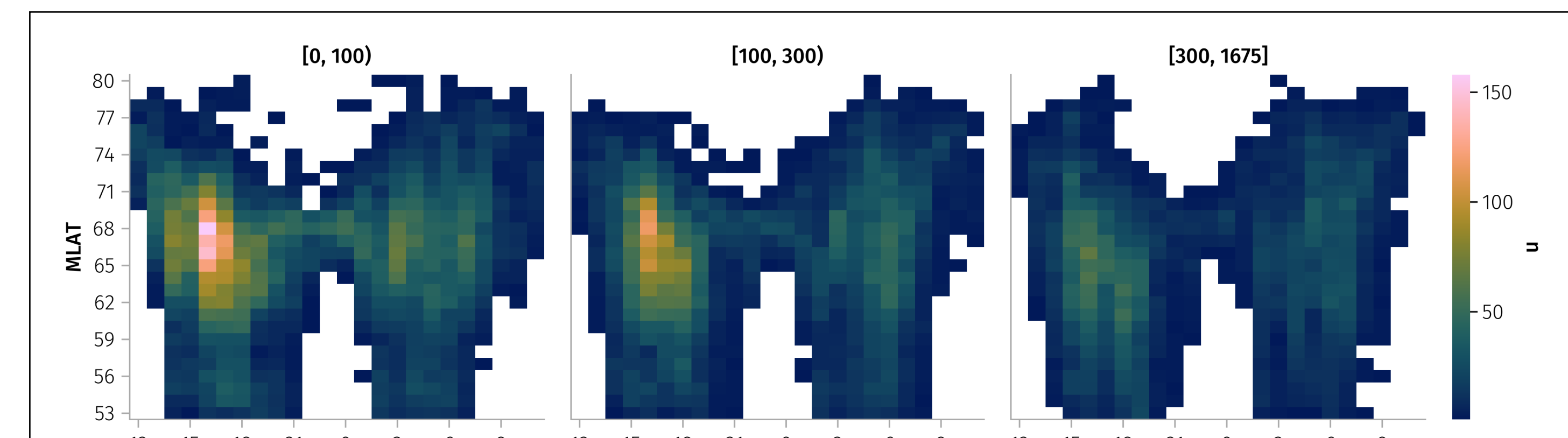


Figure 2: The total number of MLAT-averaged spectral samples across different MLT and MLAT regions, sorted the AE index.

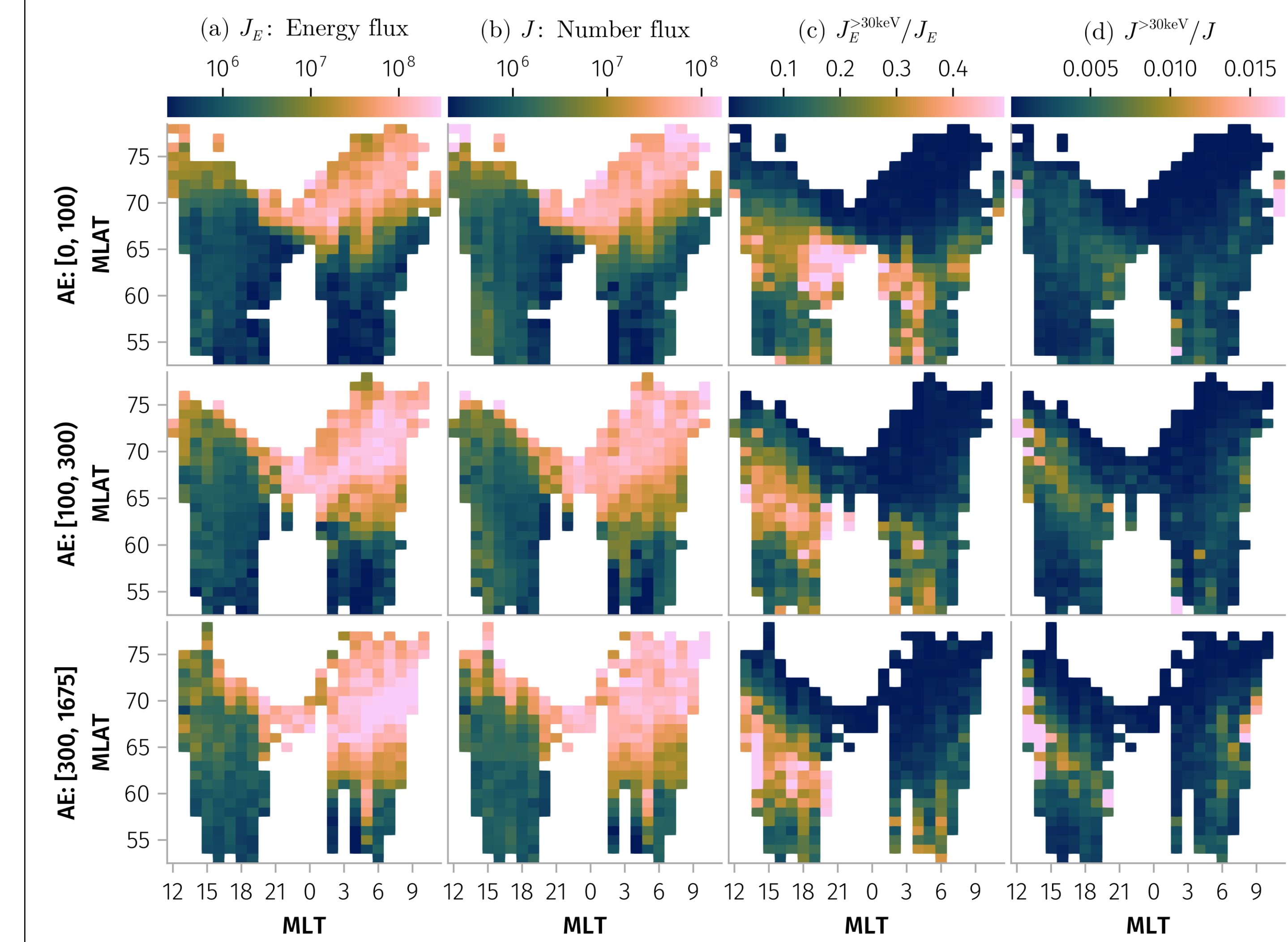


Figure 3: Median distributions of (a) total energy flux [ $\text{keV cm}^{-2} \text{s}^{-1} \text{sr}^{-1}$ ], (b) total number flux [ $\text{cm}^{-2} \text{s}^{-1} \text{sr}^{-1}$ ], and (c-d) fractional contribution of energetic particles ( $>30$  keV) to total energy and number flux.

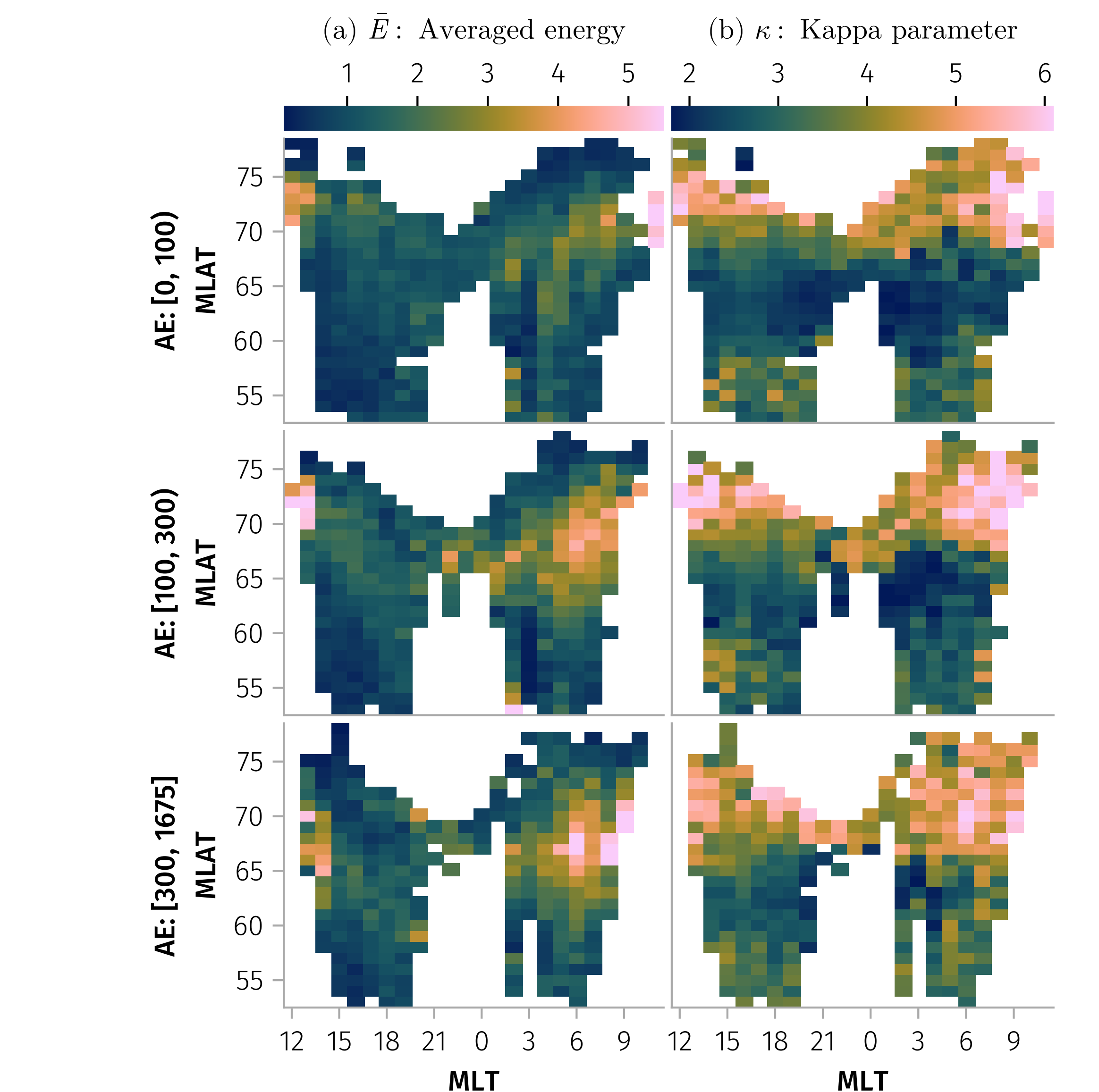


Figure 4: Median distributions of (a) averaged energy ( $\bar{E}$ ) [keV] and (b) kappa parameter ( $\kappa$ ) as functions of MLT, MLAT and AE index levels.

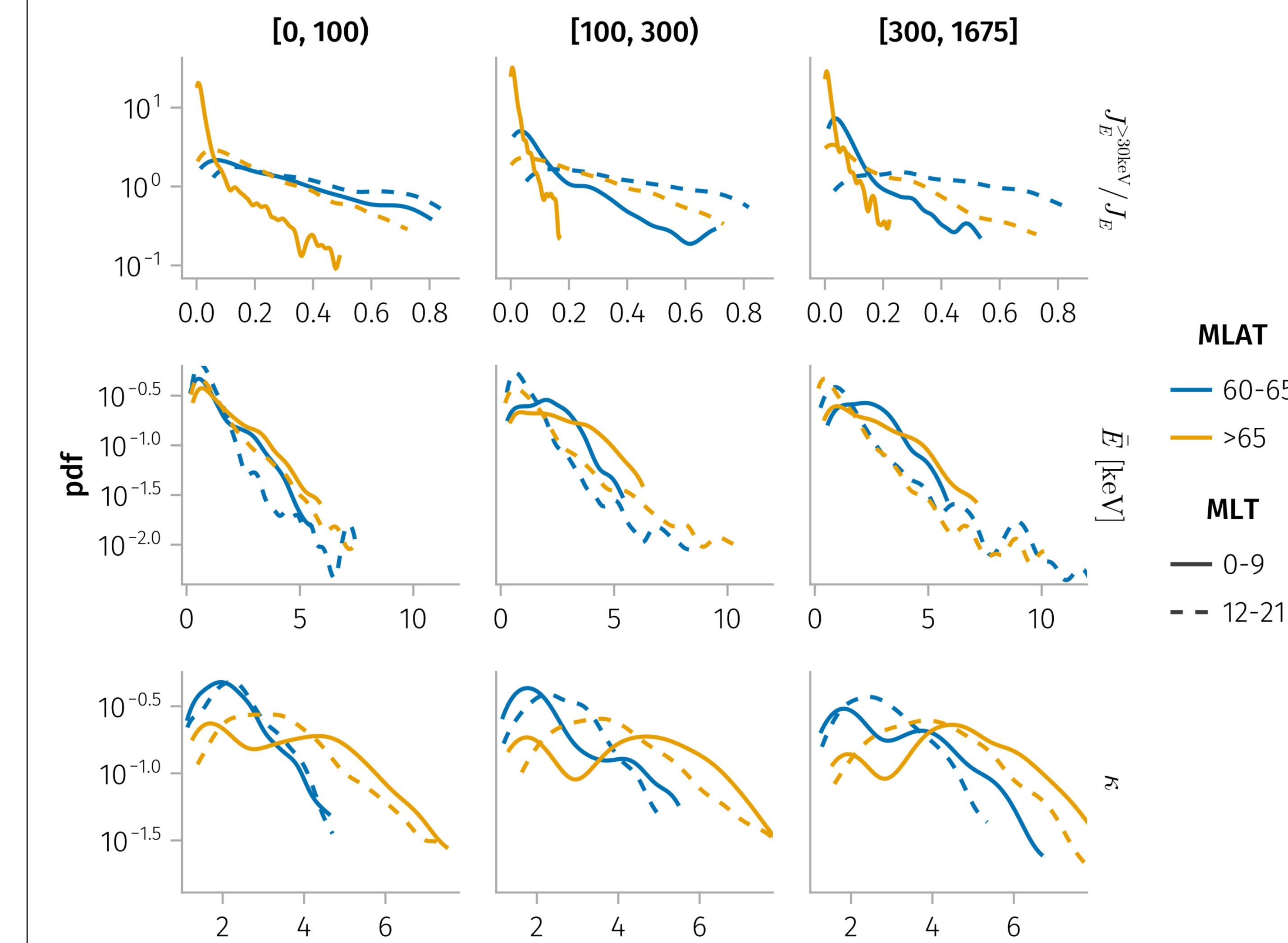


Figure 5: Probability density functions of (a) the energy flux ratio  $\frac{J_E^{>30\text{keV}}}{J_E}$ , (b) the mean energy  $\bar{E}$  [keV], and (c) the kappa parameter  $\kappa$ . Distributions are organized by three AE index ranges ( $0$ – $100$ ,  $100$ – $300$ , and  $> 300$  nT), two MLT sectors ( $12$ – $21$  and  $0$ – $9$ ), and two MLAT bands ( $60^\circ$ – $65^\circ$  and  $> 65^\circ$ ).